Submitted: July 2, 2024 **Revised: July 19, 2024** **Accepted: August 21, 2024**

Accelerated degradation by mechanical load of HIT solar cells encapsulated in flexible plastic

A.V. Bobyl [1], R.V. Davydov [2]✉, O.I. Konkov [1], A.V. Kochergin [3], D.A. Malevsky [1], S.E. Nikitin [1]

[1] Ioffe Institute, St. Petersburg, Russia

[2] Peter the Great St. Petersburg Polytechnic University, St. Petersburg, Russia

[3] STC Thin Film Technologies in Power Engineering, St. Petersburg, Russia

✉ davydovroman@outlook.com

ABSTRACT

The degradation of plastic-encapsulated silicon HIT solar cells (156 × 156 mm^2) with Ag and Cu metallization was studied under mechanical load with a soft rod with a radius of 25 mm (Ball-on-Ring) up to a maximum 400 kPa. Local 2D photo- and electroluminescence, as well as measurements of dark and light current-voltage characteristics were used. Three phases were detected: (1) an increase in power by 2 – 4 % due to a decrease in leakage currents with pressures up to 125 kPa, (2) accumulation of deformations completed by the avalanche-like formation of a volumetric defect in the substrate with a radius of up to 10 μm with a drop in power by 3 – 5 %, (3) formation of a system of cracks with a width of < 1 μm, with an increase in their total length during under maximum mechanical load to 4000 ÷ 4100 mm and a decrease in of solar cell power to 12 ÷ 16 %.

KEYWORDS

accelerated degradation • mechanical load • avalanche-like • crack • photoluminescence • electroluminescence

Citation: Bobyl AV, Davydov RV, Konkov OI, Kochergin AV, Malevsky DA, Nikitin SE. Accelerated degradation by mechanical load of HIT solar cells encapsulated in flexible plastic. *Materials Physics and Mechanics*. 2024;52(4): 1–8. http://dx.doi.org/10.18149/MPM.5242024_1

Introduction

An important area of long-term forecasting of silicon solar cell (SC) technology development is to increase their service life. In the next 10 years, according to M. Fischer, Annual report ITRPV for PV 2023, 40-year module technical lifetimes are expected. When studying the SC degradation, we will consider the following circumstances:

1. The importance of accelerated testing of materials and various devices is noted [1]. In particular, 7-day bench tests can accelerate the rate of degradation by 30 times compared to their climatic tests [1]. There is a so-called scientific direction Service Life Prediction (SLP) [2], aimed at developing new test methods for testing with an applied engineering (commercial) task to guarantee the quality of products (goods), in particular, solar modules [3].
2. According to [4], as SLP parameters become more stringent, studies can be divided into two groups: training and testing samples, which are prototypes of standard industrial standards (GOST) [5] and more detailed specialized test methods [6], respectively.
3. Among more than 50 existing SC degradation mechanisms [7], 14 % of failures occur under mechanical load and about 35 % with thermal cyclic deformations, i.e. in total, this

is almost half of the SC failures due to the mechanical damage of substrate and contact system.

4. Cracking processes are usually studied using a Ring-on-Ring bending test [8], 3 or 4 point bending tests [9].

5. Flexible silicon SC were chosen for following reasons:

5.1. They are the most widespread in the long term [7].

5.2. The market for flexible SC is expected to increase to 25 % of all SC [10].

5.3. For more effective research, it is necessary to conduct them at large deflections, as well as in the presence of SC mechanically strong protection.

Thus, standard and accelerated strength studies of SC degradation are an important stage in substantiating the reliability of their long-term forecasts. The methods must reproduce the actual operation of the solar energy system.

Materials and Methods

To obtain silicon HIT-type SC, (100) wafers (156 × 156 mm^2) of Cz-silicon produced by LONGi were used with an oxygen concentration of $8 \cdot 10^{17}$ cm^{-3}, carbon ~ $5 \cdot 10^{16}$ cm^{-3}, and a dislocation density of 500 cm^{-2}. The SC technology included: cleaning, pyramidal texturing, PECVD deposition of amorphous silicon, conductive electrodes (indium tin oxide) and the formation of Ag or Cu fingers by screen printing or electrochemical deposition, respectively [11,12]. Double-sided lamination was used with CVF film based on polyolefins (DNS company), thickness ~ 600 μm and the formation of layers of polyethylene terephthalate (PET), thickness ~ 350 ÷ 400 μm (Fig. 1).

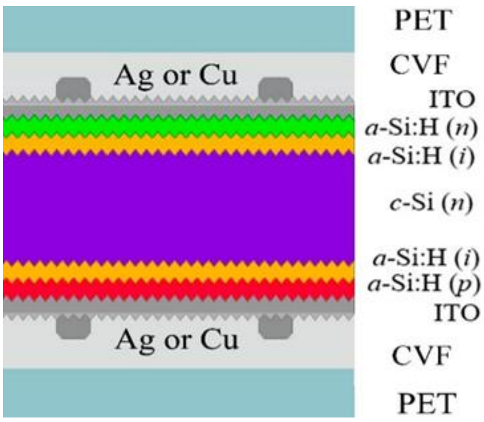

Fig. 1. Cross-section structure of HIT-type silicon SC and protective layers

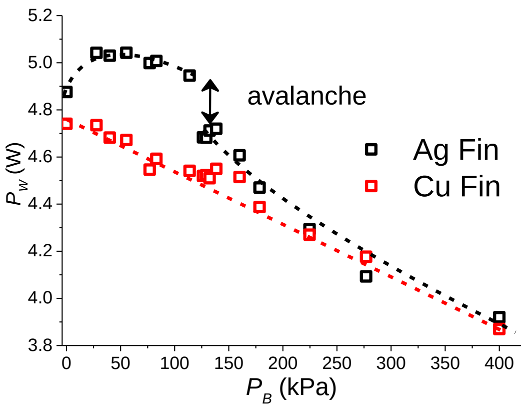

Fig. 2. Power dependences of two SC on the bending pressure P_B. The point of an avalanche-like drop in the power of SC with Ag fingers is marked

The dimensions of the laminated SC with protective layers were ~ 220 × 220 × 2.2 mm^3. They were placed in the corners on 4 supports with a soft layer thickness of 1.5 cm and an area of 2 × 2 cm^2, with a diagonal 180 mm distance between the supports. The test design followed a combination of the previously used Ball-on-Ring and Ring-on-Ring methods [8,11]. Static axial load in the range $P_B = 0 \div 400$ kPa was applied at the geometric center to the plate through $\Delta t = 200$ h to maximum P_{BM} and $t_M = 3325$ h. SC power degradation were measured on HalmcetisPV-Moduletest3 equipment at AM 1,5 (Fig. 2).

Results

EL and PL measurements

The SC were monitored at room temperature by 2D photo- and electroluminescence (PL and EL). When studying EL, external direct displacement was used. PL studies were carried out on the LumiSolarCell System (Fig. 3), and EL on the MBJ SolarModule EL-quickline 4.0 (Fig. 4).

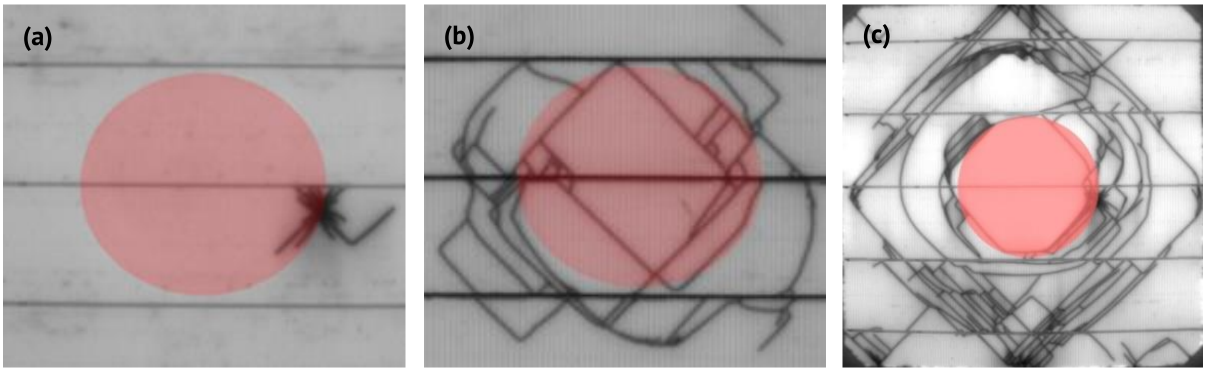

Fig. 3. (a) PL image after the occurrence of an avalanche at PB = 125 kPa in sample with Ag fingers; (b) accumulation of cracks up to PB =125 kPa in the Cu sample by fingers; (c) accumulation of cracks in the Cu sample by fingers at PBM = 400 kPa. The red disk is the pressure area

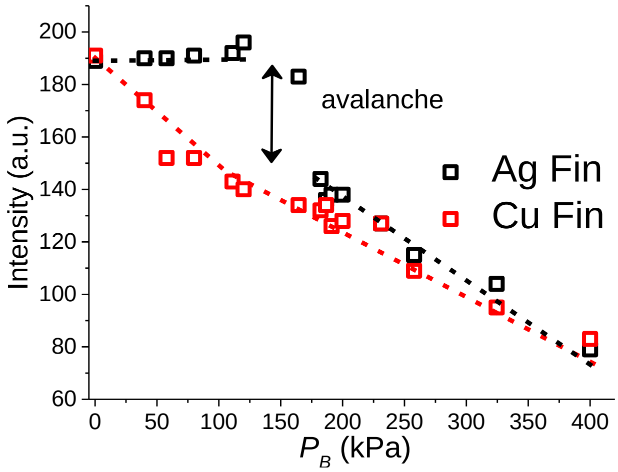

Fig. 4. Intensities EL, reduced to initial values, on the bending pressure P_B. The point of an avalanche-like drop in EL intensity of SC with Ag fingers is marked

Comparing Fig. 2 and 3 it can be seen that on the sample with Ag fingers 3 phases were detected:

1. increase in power with pressures up to 125 kPa;
2. the increase power in this sample will end with an avalanche-like appearance of a volumetric substrate defect with a radius of up to 10 μm;
3. formation of a system of cracks appearance with a width < 1 μm, and an increase in their total length at P_{BM} up to 4000 mm, and a decrease in power. On Cu finger sample, even at small P_B values, cracks appear with an increase in its total length to a slightly larger value of 4100 mm.

From Fig. 2 and 4 can be seen that for both samples their powers and EL intensities converge at large P_B, which indicates a common mechanism of SC degradation - the occurrence of cracks in the substrate.

Current-voltage characteristics measurements

According to [13], to describe degradation processes under conditions of significant changes in the current-voltage characteristics (CVC), a single-diode electrical model with series R_S and parallel R_{SH} resistances can be used. The first value will be associated with the degradation of the contact grid, and the second with parasitic leakage currents through the volume of the SC. It is obvious that measurements are necessary in both the light and dark states of SC due to significant differences in their nonlinearity. Programs for calculating dark CVC [14] and light CVC [15] have been developed using Python. In particular, dark CVCs are described by the implicit equation:

$$I = I_0 \left\{ exp\left(\frac{q(V-R_S I)}{kT}\right) - 1 \right\} + \frac{V-R_S I}{R_{SH}}. \quad (1)$$

Measurements of load and dark CVC were carried out before and after exposure to mechanical loads. The calculation results of CVC measurements are shown in Table 1.

Table 1. Power P_W (W), its changes ΔP_W (%), fill factor FF (%), R_S (ohm) and R_{SH} (ohm) SC with Ag and Cu fingers for load and dark CVC. P_B (kPa) values are indicated

Finger metals, pressure	P_W	FF	ΔP_W	Load CVC		Dark CVC	
				R_s	R_{SH}	R_s	R_{SH}
Ag							
P_B=0	4.88	73.6	0,0	0.0182	0.82	0.313	10600
P_B=100	5.04	76.36 72.34	+3.40 -0.40	0.0177	1.13 0.73	0.327	12600 156
P_B=P_{BM}	4.09	67.1	-16.1	0.0227	0.53	0.420	29.25
Cu							
P_B=0	4.74	74.0	0.0	0.0184	0.87	0.316	52.46
P_B=100	4.68	73.6	-1.24	0.0174	0.80	0.320	66.09
P_B=P_{BM}	4.18	69.4	-12.0	0.0211	0.60	0.320	57.96

Discussion

A discussion of the experimental results on the type and dependence of the number of cracks on pressure is carried out in the following sequence.

SC with Ag fingers at P_B < 125 kPa

There is an improvement in its efficiency by 3.49 %. The positive effects of heterogeneity of impurities in semiconductors are known from the work on Si p-n junctions by Goetzberger and Shockley [16] and solar silicon by Kvedera [17]. Improvements in parameters under bending loads [18], in the presence of radiation effects on GaAs [19] and Si [20], during current forming of PERC [21] and light-induced other [22,23] solar cells are also known. The ambiguity of the short-term improvement of the latter in [24] is associated with the presence of a starting "infant" stage of operation, in particular at this stage there is a rapid significant drop in power up to 5 % [7].

SC with Ag Fingers at P_B ~ 125 kPa

The appearance of a large dendrite-like [7] or cross-like [25] crack system can be explained by the presence of elastic energy accumulation stag and its avalanche-like release. A volumetric substrate defect with a radius of up to 10 μm is formed with a 4 % power drop. Only the mechanism of internal avalanche corrosion is possible [26] due to two reasons: 1) under our experiment conditions, the so-called Sustained-load cracking or delayed fracture (pressure is applied and a significant delay with its subsequent increase) [27,28], 2) experimental temperatures are much lower than Si brittle-to-ductile transition temperatures (~ 550 °C) [29]. This mechanism was also previously observed during the embrittlement of metals with hydrogen [27], in brittle solids [30], and in Si at high temperatures [31].

SC with Cu fingers at P_B from 0 to P_{BM}, SC with Ag fingers at P_B > 125 kPa and up to P_{BM}

As can be seen from Fig. 3(c), two areas can be distinguished: near the pressure application contour and at its periphery. Usually, images of curved and rounded cracks are observed [7,32], and much less often cases are observed with a change in the angle of their growth by 90° [33], which is associated with the anisotropy of the potential at the end of the crack [34]. The presence of this anisotropy is probably important for the formation of the small rectangular shapes that we observed, but for the large rounded squares, a more likely reason is the corresponding symmetry of the strain distribution [35]. In general, the length of the cracks and the nature of their growth as the pressure increases are fully consistent with the Sustained-load cracking and brittle fracture of metals methods described and consisting of 3 stages [36,37]: the occurrence of cracks, their growth and destruction of the sample. At the same time, for SC, the presence of a large number of cracks and a power drop of up to 10 % for several solar cells in a module is considered quite acceptable in conditions of mass industrial production [38–40].

Conclusion

The usefulness and reliability of the results of studies of SC degradation mechanisms is largely determined by their methodology and its proximity to real operating conditions. The following circumstances are important:

1. carrying out accelerated degradation in accordance with the concept of Service Life Prediction (SLP) [3];
2. testing in a wide range of external influences;
3. conducting strength tests because in total, this is almost half of the SC failures due to the mechanical damage of substrate and contact system;
4. for more effective research is necessary to conduct them on flexible SC.

The following results were obtained:

1. Three phases of power changes were detected: (i) an increase in SC power by 2–4 % at low pressure, (ii) accumulation of deformations completed by the avalanche-like substrate damage with a drop in power by 3–5 %, (iii) formation of crack system with an

increase in their total length at P_{BM} to 4000 ÷ 4100 mm and a decrease in of SC power to 12 ÷ 16 %.
2. The ambiguity of the short-term SC power improvement is associated with the presence of a starting "infant" effect.
3. The appearance of a large dendrite-like or cross-like crack system can be explained by the presence of elastic energy accumulation stage and its avalanche-like release.
4. For both SC samples with Ag and Cu fingers their powers and EL intensities converge at large P_B, which indicates a common mechanism of SC degradation - the occurrence of cracks in the substrate.
5. The factor for accelerating degradation (AD) by ML using developed method can be calculated within the range AD = 25 ÷ 50.
6. Combined Ball-on-Ring and Ring-on-Ring scheme made it possible to carry out accelerated degradation of solar cells parameters by 12 ÷ 16 % in 140 days, close to corresponding degradation values over 10–20 years of their operation in natural (field) conditions.
7. The use of local 2D photo- and electroluminescence methods, measurements of dark and light (load) current-voltage characteristics make it possible to fully describe the degradation processes of both the SC electric contact grid and the volume of the active photovoltaic part of the SC.

References

1. Nelson HA, Schmutz FC. Accelerated weathering. A consideration of some fundamentals governing its application. *Trans. Roy. Soc. London*. 1926;18(12): 1222–1227.
2. Martin JW, Ryntz RA, Chin J, Dickie RA. (eds.) *Service life prediction of polymeric materials: global perspectives*. Springer; 2009.
3. Jordan DC, Kurtz SR. *Photovoltaic degradation rates: an analytical review*. National Renewable Energy Laboratory; 2012.
4. James G, Witten D, Hastie T, Tibshirani R. *An Introduction to Statistical Learning with Applications*. NY: Springer; 2013.
5. Standard IEC. IEC 61215-1-1:2021. *Terrestrial photovoltaic (PV) modules - Design qualification and type approval- Part 1: Test requirements*. International Electrotechnical Commission; 2021.
6. Standard MIL-STD-810H. *Environmental engineering considerations and laboratory tests*. 2014.
7. Köntges M, Kurtz S, Packard CE, Jahn U, Berger KA, Kato K, Friesen T, Liu H, Van Iseghem M, Wohlgemuth J, Miller D, Kempe M, Hacke P, Reil F, Bogdanski N, Herrmann W, Buerhop-Lutz C, Razongles G. Friesen G. *Review of failures of photovoltaic modules*. Report IEA-PVPS T13-01:2014, 2014.
8. Nikitin SE, Shpeizman VV, Pozdnyakov AO, SI Stepanov, RB Timashov, VI Nikolaev, Terukov EI, Bobyl AV. Fracture strength of silicon solar wafers with different surface textures. *Materials Science in Semiconductor Processing*. 2022;140: 106386.
9. Borrero-Lopez O, Vodenitcharova T, Hoffman M, Leoz AJ Fracture strength of polycrystalline silicon wafers for the photovoltaic industry. *J. Am. Ceram. Soc.* 2009;92(11): 2713–2717.
10. Li X, Li P, Wub Z, Luo D, Yu HY, Lu ZH. Review and perspective of materials for flexible solar cells. *Materials Reports: Energy*. 2021;1(1): 100001.
11. Abolmasov S, Kochergin A, Terukov EI, Shelopin G. Conducting climatic and mechanical tests for solar modules made of heterojunction PV cells with a copper contact grid. *Adv. Eng. Res.* 2022;213: 39–44.
12. Shetty DK, Rosenfield AR, McGuire P, Bansal GK, Duckworth WH. Biaxial flexure test for ceramics. *Amer. Ceramics Soc. Bull.* 1980;59(12): 1193–1197.
13. Humada AM, Hojabri M, Mekhilef S, Hamada HM. Solar cell parameters extraction based on single and double-diode models: A review. *Renewable and Sustainable Energy Reviews*. 2016;56: 494–509.
14. Würfel P, Würfel U. *Physics of Solar Cells*. Wiley-VCH Verlag GmbH & Co; 2016.

15. Celik AN, Acikgoz N. Modelling and experimental verification of the operating current of mono-crystalline photovoltaic modules using four- and five-parameter models. *Applied Energy*. 2007:84(1): 1–15.
16. Goetzberger A, Shockley W. Metal precipitates in Silicon pn junctions. *J. Appl. Phys*. 1960;31: 1821–1824.
17. Kveder V, Schroter W, Sattler A, Seibt M. Simulation of Al and phosphorus diffusion gettering in Si. *Materials Science and Engineering*. 2000;71(1-3): 175–181.
18. Sawada R, Karaki T, Watanabe J. Gettering of crystalline defects in Si by bending. *Applied Physics Letters*. 1981;38: 368–369.
19. Grusha SA, Evstigneev AM, Ismailov KA, Konakova RV, Krasiko AN, Sinishchuk IK, et. al. Electric field effect on radiation-induced gettering of defects in GaAs. *Phys. Stat. Sol. (A)*, 1984;86(1): 83–87.
20. Zhang Y, Qin L, Hou R, Ma N, He Y, Chen X, Yao L, Xu W, Qin G. Room-temperature gettering of Au in Si wafers with surface defects under small dose γ-ray radiation. *J. Phys. D: Appl. Phys.* 2015;48: 105101.
21. Wang Z, Shen H, Hu D, Wei Q, Ni Z, Li Y, Sun L, Qian H. Influence of double current injection annealing on anti-LID effect in mono-like silicon PERC solar cells. *Journal of Materials Science: Materials in Electronics*. 2020;31: 3221–3227.
22. Wright M, Stefani BV, Soeriyadi A, R Basnet, C Sun, W Weigand, Z Yu, Z Holman, Macdonald D, Hallam B. Progress with Defect Engineering in Silicon Heterojunction Solar Cells. *Physica Status Solidi (RRL)*. 2021;15(9): 2100170.
23. Boudjemila L, Davydov VV, Aleshin AN, VM Malyshkin, EI Terukov. Electrical characteristics of CsPbI3 and CsPbBr3 lead halide Pervoskvite nanocrystal films deposited on Si-c solar cells for high-efficiency photovoltaics. *St. Petersburg State Polytechnical University Journal: Physics and Mathematics*. 2022;15(3.2): 91–96.
24. Madumelu C, Wright B, Soeriyadi A, Wright M, Chen D, Hoex B, Hallam B. Investigation of light-induced degradation in N-type silicon heterojunction solar cells during illuminated annealing at elevated temperatures. *Solar Energy Materials and Solar Cells*. 2020;218: 110752.
25. Köntges M, Morlier A, Eder G, Fleiß E, Kubicek B, Lin J. Review: ultraviolet fluorescence as assessment tool for photovoltaic modules. *IEEE Journal of Photovoltaics*, 2020, 10(2): 616–633.
26. Segbefia OK, Akhtar N, Sætre TO. Moisture induced degradation in field-aged multicrystalline silicon photovoltaic modules. *Solar Energy Materials and Solar Cells*. 2023;258: 112407.
27. Landes JD, Wie RP. The kinetics of subcritical crack growth under sustained loading. *International Journal of Fracture*. 1973;9(3): 277–293.
28. Storgärds E, Simonsson K. Crack length evaluation for cyclic and sustained loading at high temperature using potential drop. *Experimental Mechanics*. 2015;55(3): 559–568.
29. Samuels J, Roberts SG, Hirsch PB. The brittle-to-ductile transition in silicon. *Materials Science and Engineering: A*. 1988;105–106(1): 39–46.
30. Barés J, Bonamy D. Crack growth in heterogeneous brittle solids: intermittency, crackling and induced seismicity. *Phil. Trans. R. Soc. A*. 2019;377(2136): 20170386.
31. Tanner BK, Garagorri J, Gorostegui-Colinas E, Elizalde MR, Bytheway R, McNally PJ, Danilewsky AN. The geometry of catastrophic fracture during high temperature processing of silicon. *Int J Fract*. 2015;195: 79–85.
32. Papargyri L, Theristis M, Kubicek B, Krametz T, Mayr C, Papanastasiou P, Georghiou GE. Modelling and experimental investigations of 1 microcracks in crystalline silicon photovoltaics: A review. *Renewable Energy*. 2020;145: 2387–2408.
33. Dhimish M, Hu Y. Rapid testing on the effect of cracks on solar cells output power performance and thermal operation. *Sci Rep*. 2022;12: 12168.
34. Alam MS, Wahab MA. A new approach for modeling of fatigue crack growth in welded cruciform and curve T joint structures. In: *ASME 2005 International Mechanical Engineering Congress and Exposition*. ASME; 2008. p.351–360.
35. Espitia-Mesa G, Hernández-Pedraza E, Molina-Tamayo S, Mejía-Gutiérrez R. Design, analysis, and modeling of curved photovoltaic surfaces using composite materials. *TecnoLógicas*. 2022;25(53): e2171.
36. Liu D, Pons DJ. Crack propagation mechanisms for creep fatigue: a consolidated explanation of fundamental behaviours from initiation to failure. *Metals*. 2018;8(8): 623.
37. Köntges M, Kunze I, Kajari-Schröder S, Breitenmoser X, Bjørneklett B. The risk of power loss in crystalline silicon based photovoltaic modules due to micro-cracks. *Solar Energy Materials and Solar Cells*, 2011;95(4): 1131–1137.
38. Morlier A, Haase F, Köntges M. Impact of cracks in multicrystalline silicon solar cells on PV module power - a simulation study based on field data. *IEEE Journal of Photovoltaics*. 2015, 5(6): 1735–1741

39. Boudiemila L, Davydov V, Malyshkin V. Quantum-mechanical methods for processing the results of classical experiments as an alternative to kalman filter. In: *Proceedings of the 2021 International Conference on Electrical Engineering and Photonics*. EExPolytech; 2021. p.256–259.
40. Rud V, Melebaev D, Krasnoshchekov V, Ilyin I, Terukov E, Diuldin M, Andreev A, Shamuhammedowa M, Davydov V. Photosensitivity of nanostructured Schottky barriers based on GaP for solar energy applications. *Energies*. 2023;16(5): 2319.

About Authors

Alexander V. Bobyl Sc
Doctor of Physical and Mathematical Sciences
Leading Researcher (Ioffe Institute, St. Petersburg, Russia)

Roman V. Davydov Sc
Candidate of Physical and Mathematical Sciences
Associate Professor (Peter the Great St. Petersburg Polytechnic University, St. Petersburg, Russia)

Oleg I. Konkov Sc
Candidate of Physical and Mathematical Sciences
Senior Researcher (Ioffe Institute, St. Petersburg, Russia)

Artem V. Kochergin Sc
Technologist (STC Thin Film Technologies in Power Engineering, St. Petersburg, Russia)

Dmitry A. Malevsky Sc
Senior Researcher (Ioffe Institute, St. Petersburg, Russia)

Sergey E. Nikitin Sc
Candidate of Chemical Sciences
Senior Researcher (Ioffe Institute, St. Petersburg, Russia)